DEVELOPMENT OF A NOVEL UWB VIVALDI ANTENNA ARRAY USING SIW TECHNOLOGY

S. Lin, S. Yang, and A. E. Fathy

EECS Department
University of Tennessee
1508 Middle Drive, Knoxville 37996, TN, USA

A. Elsherbini

ECE Department
Ain Shams University
Cairo, Egypt

Abstract—A compact Vivaldi antenna array printed on thick substrate and fed by a Substrate Integrated Waveguides (SIW) structure has been developed. The antenna array utilizes a compact SIW binary divider to significantly minimize the feed structure insertion losses. The low-loss SIW binary divider has a common novel Grounded Coplanar Waveguide (GCPW) feed to provide a wideband transition to the SIW and to sustain a good input match while preventing higher order modes excitation. The antenna array was designed, fabricated, and thoroughly investigated. Detailed simulations of the antenna and its feed, in addition to its relevant measurements, will be presented in this paper.

1. INTRODUCTION

The concept of SIW technology was first proposed in 1994 [1]. SIW technology makes it possible to realize the waveguide in a substrate and provides an elegant way to integrate the waveguide with microwave and millimeter wave planar circuits using the conventional low-cost printed circuit technology. Since its inception, a vast range of SIW components, such as filters, phase shifters, transitions, couplers, power dividers, and diplexers, have been proposed and studied [2–6].
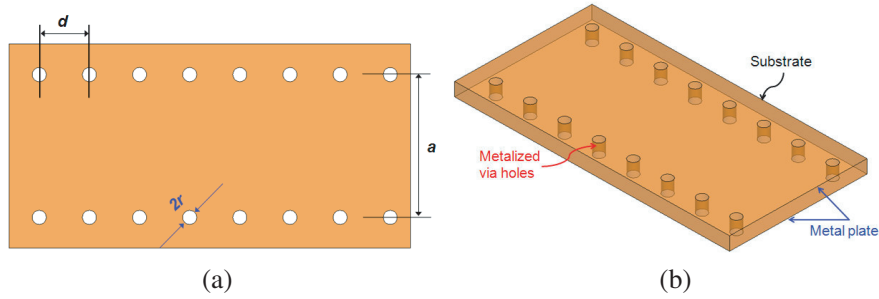
Corresponding author: S. Lin (slin1@utk.edu).

(a)   (b)

Figure 1. Substrate integrated waveguide on dielectric substrates: (a) Top view; (b) 3D view.

SIW structures are fabricated on printed circuit boards. Its emulated waveguide SIW sidewalls are constructed from lined via-holes rather than the solid fences used in conventional metallic waveguides, as shown in Figure 1. This technology is simple, less expensive than its predecessors, and even renders light structures. Yang et al. [7] presented an extensive full parametric study of the SIW structures based on a full-wave, 3D analysis using Ansoft HFSS [8]. In this paper, we utilize this technology to develop a Vivaldi wideband antenna array with a relatively low insertion loss.

Ultra-wideband (UWB) antennas are a class of broadband antennas with considerably wide bandwidths. Following is a definition for UWB antennas, according to their impedance bandwidths, communicated by the Federal Communications Commission (FCC). An antenna whose minimum operating frequency is f_L and whose highest operating frequency is f_H can be classified as an UWB antenna if

$$FBW = 2\frac{f_H - f_L}{f_H + f_L} > 0.2 \quad \text{or} \quad BW = f_H - f_L > 500\,\text{MHz}$$

where FBW is the fractional bandwidth of the antenna.

When compared with conventional narrow-band systems, it is challenging to design an antenna for an UWB system. Therefore, trade-offs are generally made between wide bandwidth, good input match, compact size, low-cost, high radiation efficiency, and minimal dispersion.

Table 1 summarizes the characteristics of different UWB antennas. The Vivaldi antenna belongs to the tapered slot antennas (TSA) class and there are good candidates for wide band performance. The Vivaldi antennas are extremely suitable for UWB antenna applications due to their varied features. The features include a high gain, simple

design, narrow beam width in the E-plane, and a relatively wide operating bandwidth. The Vivaldi antennas do not necessitate wide lateral dimensions easing manufacturing [9]. The Vivaldi antenna have been used in several UWB applications such as See-Through-Wall Imaging [10], Indoor Localization Systems [11], and Breast Tumor Detection [12]. However, their overall performance is generally hindered by the need for a wideband feeding network.

Table 1. UWB antenna characteristics.

Type	Bandwidth	Gain	Size	Cost
Crossed Monopole	Wide	Low	Small	Low
Conical	Wide	Medium	Medium	High
Bowtie	Wide	Medium	Small	Low
TEM	Wide	Medium	Bulky	High
Taper Slot (Vivaldi)	Wide	High	Medium	Medium

As the antenna's feed network can cause significant insertion loss, we propose to develop a wideband Vivaldi antenna array utilizing low-cost SIW technology. Our design addresses the following design challenges:

1) Compact, low loss, wideband feeding network
2) Wideband SIW to the connector transition
3) Wideband Vivaldi antenna.

Similar efforts to develop low-loss wide band antennas have been previously performed. For example, Yang et al. [13] developed an UWB Vivaldi antenna to cover the 8–12 GHz bandwidth, but was based on the microstrip technology and demonstrated an overall, substantially high, insertion loss (over 3.5 dB). Additionally, Hao et al. [14, 15] utilized a SIW binary feed network with improved performance, but its 2.5 dB insertion loss is still inadequate for high performance receivers. Recently, Yang et al. [16] has developed an elegant and efficient SIW feed network for a slotted array antenna for DBS applications, which has led to significant performance improvements. A thicker substrate was used to reduce the conductor loss, and to develop an optimized GCPW feed to the binary SIW structure to improve both the bandwidth and return loss performance. This prevents the excitation of higher order modes normally associated with the use of microstrip lines on thick substrates. This novel design will be adapted here in our UWB Vivaldi antenna development.

Our proposed antenna array consists of three parts: (1) an array of eight printed radiating elements (Vivaldi antenna) placed along the
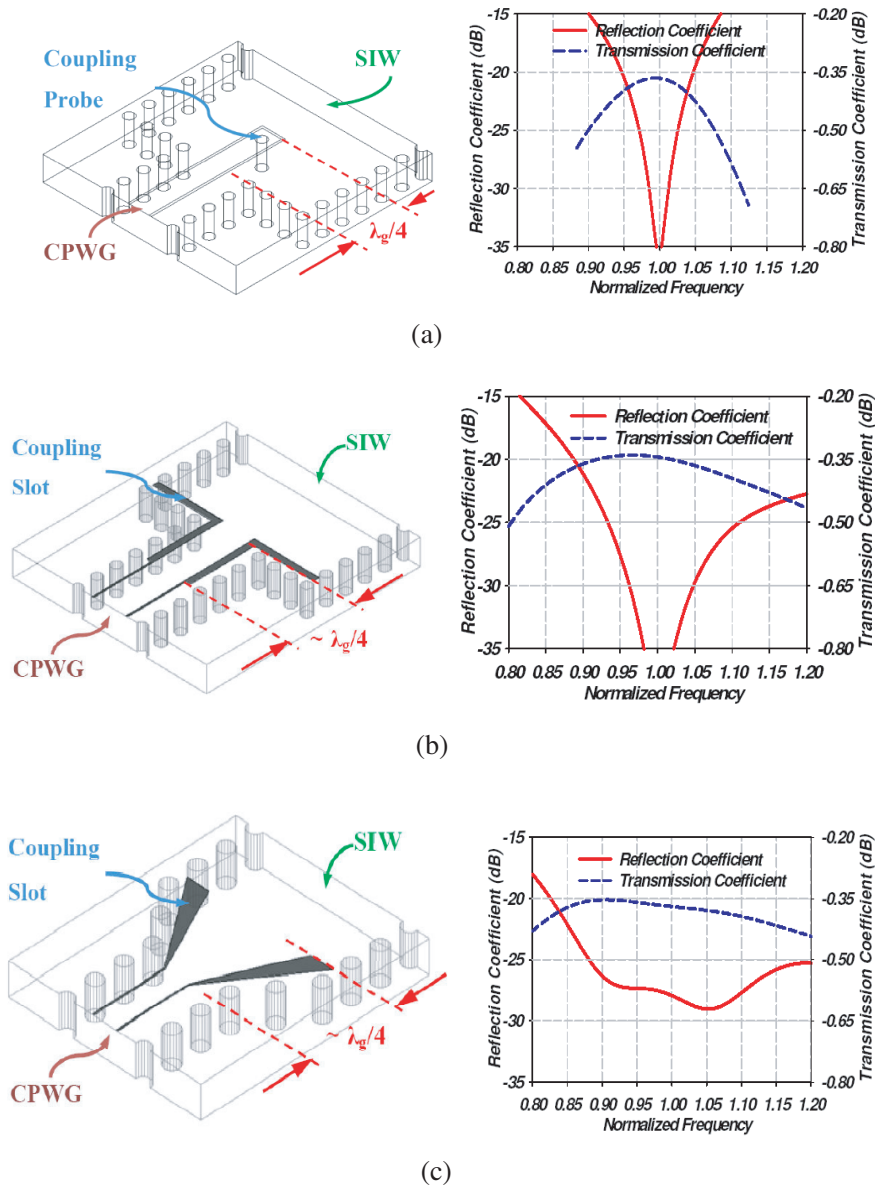
(a)

(b)

(c)

Figure 2. GCPW to SIW transitions: (a) Current probe; (b) Magnetic dipole slot; (c) Triangle coupling slot.

axis, (2) a feeding network printed on the same dielectric substrate with the radiating elements, and (3) a wideband SIW to the connector transition. Design details of the proposed wideband transitions and feeding networks, together with the simulations and experimental results of the fabricated structure, will be presented in the following sections.

2. DESIGN OF WIDEBAND GCPW TO SIW TRANSITION

In our design, we used a relatively large thickness of the substrate where a GCPW has to be employed to prevent the excitation of higher order modes, present if a conventional microstrip line is used. A current probe transition (H-field coupling) from the grounded coplanar waveguide (GCPW) to SIW is proposed by [17]. As shown in Figure 2(a), a plated through hole is placed in the junction to operate as a current coupling probe. To insure a full power transfer, the GCPW is terminated by an open circuit next to the coupling probe, where the current flowing through the probe generates a magnetic field that has similar distribution to that of the H-field of the TE_{10} mode in the SIW. In addition, via holes are strategically placed along the GCPW to cancel the parallel plate mode in the GCPW line, and to cut off the waveguide modes entering the GCPW from the SIW.

Alternatively (as shown in Figure 2(b)), Patrovsky et al. [18] proposed a CPWG to SIW transition using an E-field coupling. The coupling slots are cut on the top surface of the SIW and placed next to the short circuit termination of the SIW. The coupling slots act like a magnetic dipole antenna with a strong E-field across the slot in the center, but weaker on the end of the slot. Such distribution matches the E-field distribution of the TE_{10} mode in the SIW structure, and a smooth transition can be achieved. However, the impedance transformer still limits bandwidth. An even wider transition bandwidth can be achieved by integrating the coupling slot and the impedance transformer into one tapered coupling slot. As shown in Figure 2(c), the sidewalls of the SIW are tapered along the triangle-shaped coupling slot in such a way that the direction of the electric field on the coupling slot is always perpendicular to the SIW sidewalls. This allows for a smooth transition. The tapered coupling slot also serves as an impedance transformer to transform any arbitrary impedance line in SIW to the CPWG port impedance. As shown on the right side of Figure 2, the normalized simulation results indicate a significant bandwidth improvement with the proposed triangle slot transition.

Additionally, in the previous implementation of this transition [18, 19], an SMA connector was utilized and no design details were given. However, in this case, due to the use of a thicker substrate to reduce the feed network losses, the employment of regular SMA connectors at the input feed port would not be practical. Therefore, the GCPW to SIW transition has been re-optimized to include an N-Type connector instead of the SMA, as shown in Figure 3(a). It was determined that the optimized length of the taper slot is quarter-wave length of the center frequency to achieve a wider bandwidth. A back-to-back transition was fabricated, shown in Figure 3(b). The measured results show that the designed transition operates over a bandwidth of 2 GHz with an insertion loss of less than 0.7 dB. This is slightly higher than the simulation results using Ansoft HFSS, shown in Figure 3(c).
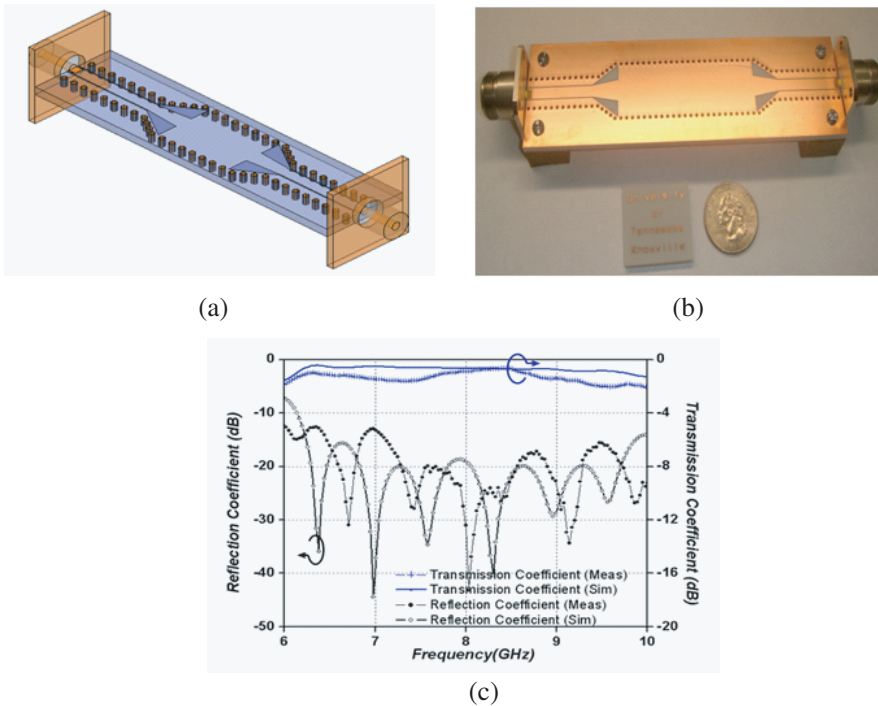

(a)   (b)

(c)

Figure 3. (a) N-Type connector to SIW back to back transitions model in Ansoft HFSS; (b) Manufactured GCPW to SIW back to back transitions; (c) Simulated and measured results.

3. DESIGN OF FEEDING NETWORK

The developed binary feed network construction is based on the extensive use of optimized compact T-junction designs. Basic rules of T-junction designs were previously developed by [20] through direct translation from its metallic waveguide version [21, 22] to SIW, as shown in Figure 4(a). In this implementation, an equivalent "a" dimension of SIW has been selected to give a relatively wide bandwidth for a single stage T-junction, as well as an acceptable insertion loss. Next, the spacing between the combining stages was judiciously selected to achieve a wideband, compact, 1 to 8 power divider in three stages connected in cascade, shown in Figure 4(b). A backtoback 1 to 8 power divider was fabricated as shown in Figure 4(c). The divider is extremely compact and its measured back-to-back insertion loss from 7.5 to 8.5 GHz is less than 2.5 dB This insertion loss is much lower than similar measurements reported by [14, 15]. As mentioned in [18], this type of SIW feeding network can provide a balanced power division over a wide band. Both the balanced power split and low insertion loss should assist with increasing the gain and overall efficiency of the antenna array. Meanwhile, the use of thick substrates and optimized T-junctions has created an improvement in performance. At the same time, the input port has a commendable return loss over the 7 to 9 GHz frequency range. Figure 4(d) shows the reflection coefficient and the transmission coefficient of the structure shown in Figure 4(c).

4. SINGLE ANTENNA ELEMENT DESIGN

Utilizing SIW technology, a number of UWB antenna structures can be used. Included are H-plane horns, slot antennas, tapered-slot traveling wave antennas, etc. H-plane horns would require extremely thick substrates in order to achieve a low return loss over a wideband. This would increase the system's overall cost. Meanwhile, slot antennas have the advantage of being small and can be used in a traveling wave array configuration to form a 2D-array. However, the differential phase shift between the elements will change with frequency, causing a beam squint. To have the beam direction constant with frequency, SIW feeding tapered slot antennas have been chosen. The utilized taper can be linear (LTSA), exponential (Vivaldi), elliptical, or constant width (CWTSA) [23]. Linear elements are generally easier to design due to the relatively small number of parameters that need to be optimized. However, the elements need to be long enough to be a good match over a wideband, as described in [15], where an 80 mm taper length was utilized. Instead of using the wideband balun, a SIW has been employed to feed a Vivaldi antenna.
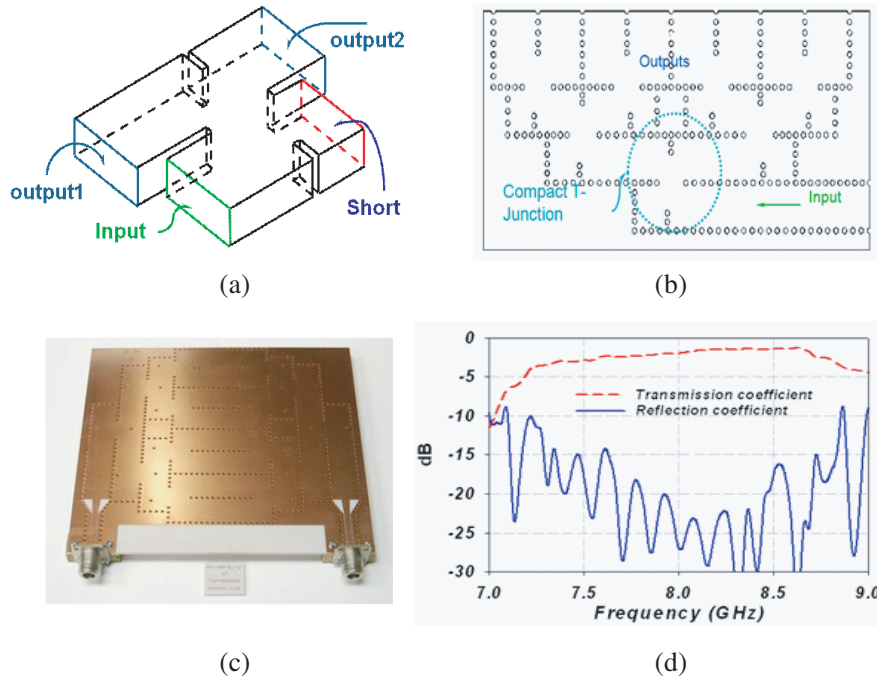
(a)

(b)

(c)

(d)

Figure 4. (a) Compact T junction; (b) Compact 1 to 8 power divider layout; (c) Back-to-back 1 to 8 feeding network; (d) Measured reflection coefficient and transmission coefficient of the back-to-back 1 to 8 feeding network.
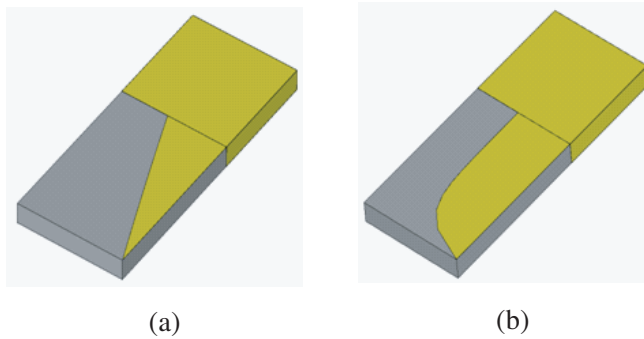

(a)   (b)

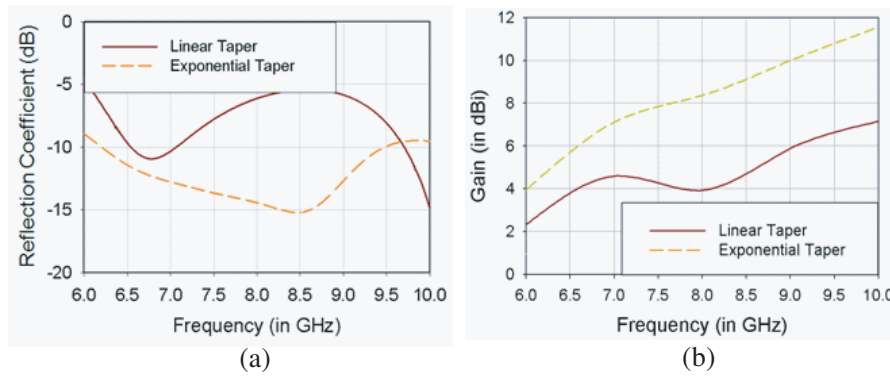**Figure 5.** The two investigated elements: (a) Linearly tapered slot antenna; (b) Exponentially tapered slot antenna.

(a)   (b)

Figure 6. (a) Reflection coefficients of the two elements; (b) Gains of the two elements.

$$C_1 = \frac{w1 + ws}{2}\left(e^{r \bullet l\_taper} - 1\right)$$

$$C_2 = -\frac{ws + w1 \bullet e^{r \bullet l\_taper}}{2}\left(e^{r \bullet l\_taper} - 1\right)$$

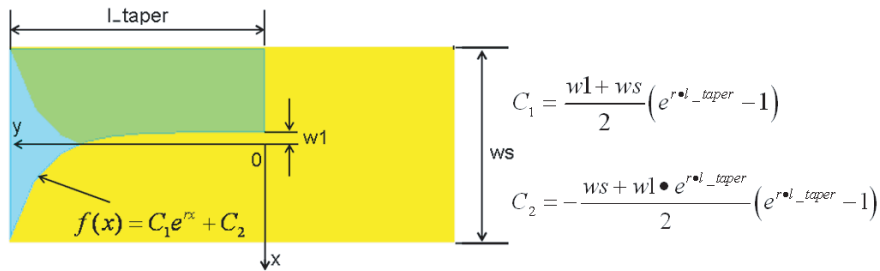**Figure 7.** Configuration of the proposed antipodal Vivaldi antenna.
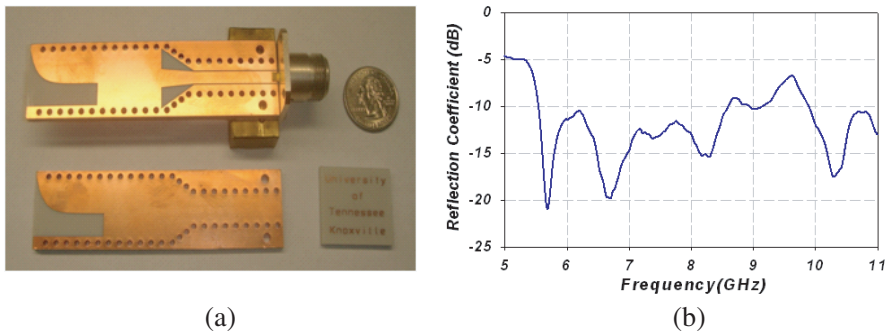

(a)   (b)

Figure 8. (a) Fabricated single element; (b) Measured reflection coefficient.

Two configurations have been investigated (shown in Figure 5). For a compact and wide band operation, the taper lengths selected were 27 mm. The first element is a LTSA. The LTSA demonstrated an acceptable return loss, but only covered a narrow band. The second element is an exponentially tapered element, whose taper rate was optimized to obtain a low return loss. Over a 10 dB return loss was achieved in simulation, as shown in Figure 6(a). Figure 6(b) indicates that a higher gain can be achieved by using exponentially tapered element. The design detail of the single element is shown in Figure 7. Its dimensions are shown in Table 2. Figure 8(a) shows the fabricated single element Vivaldi antenna. Figure 8(b) indicates that the measured return loss of the single element Vivaldi antenna is less than 10 dB over the 5.5 to 9 GHz frequency range.

Table 2. Parameters of the single element.

l_taper (mm)	r	$w1$ (mm)	ws (mm)
27	0.3	1.25	20.5

5. EIGHT ELEMENTS ARRAY DESIGN

In designing an eight element array, requirements include a small return loss, high gain, and minimum structure losses (i.e., achieve high radiation efficiency) to reduce the antenna noise temperature, and obtain a high G/T ratio. An E-plane uniform distribution, with a binary feed network, has been chosen to allow a uniform excitation over the required wideband. The gain of the array vs. elements spacing is plotted in Figure 9(a). Note that the gain of the array increases as the elements spacing increases until the spacing is near 0.9λ, and then, it drops quickly. This occurs because of the appearance of grating lobes which reduce the overall gain of the array and noticeably increase the side lobe level up to 0 dB, as shown in Figure 9(b). The optimum design would be to set the spacing between the elements to $\sim 0.8\lambda$ at the highest operating frequency (λ_{min}). No grating lobes would then appear over the operating band while achieving the maximum possible gain. Also, the increase in the gain vs. frequency is partially compensated for by an increase of the conductor and dielectric losses, which also increases with frequency, allowing a better fidelity over the operating band.

Another point to consider in this array design is the mutual coupling between the elements which affects the return loss of the single element when it is placed in an array configuration. The

structure used for evaluating the mutual coupling between the elements is shown in Figure 10(a), where three elements are placed next to each other while one element is excited. As shown in Figure 10(b), the reflection coefficient of the center element (S_{22}) was only slightly less than $-5\,$dB due to the mutual coupling from adjacent elements. Increasing the spacing between the elements can be used to reduce the mutual coupling effect. However, it will enlarge the size of the overall array and may cause the appearance of a grating lobe near the high frequency end of the band. An alternative approach, to significantly reduce the mutual coupling effects, is to extend the waveguide side walls to the end of the tapered slot antenna. Subsequently, as shown in Figure 10(b), the reflection coefficient can be greatly improved while the mutual coupling effect is significantly reduced.
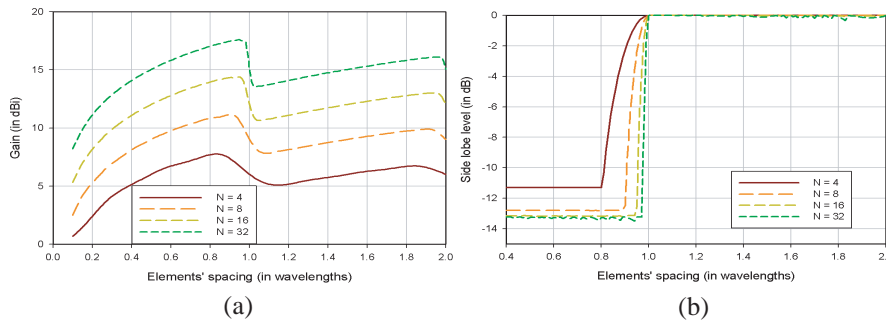

(a)   (b)

Figure 9. (a) Gain of the array vs. elements spacing; (b) Side lobe level vs. elements spacing (includes the SLL of the grating lobe).
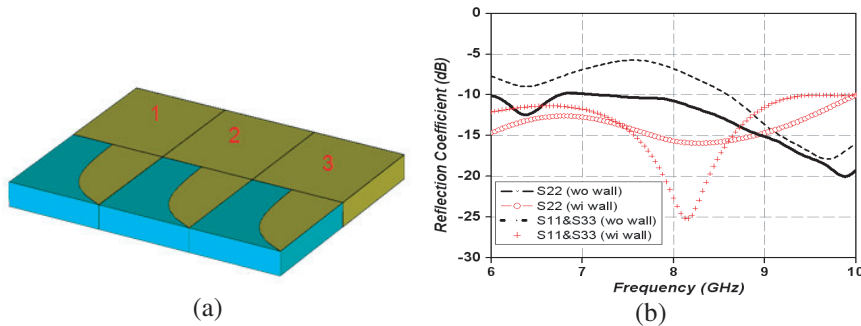

(a)   (b)

Figure 10. (a) Three element test structure for the mutual coupling effect; (b) Reflection coefficient of each element before and after adding the side walls.

The Vivaldi antenna array is designed and fabricated to operate over a 7 to 9 GHz frequency range. It was printed on a 125 mil thick Neltec NY9208 substrate with a dielectric constant of 2.08 and a loss tangent of 0.0006. Figure 11 shows the manufactured eight-element Vivaldi array, where eight Vivaldi antenna elements are fed using a SIW structure feeding network.

6. ARRAY MEASUREMENTS

The measured input return loss and radiation patterns are shown in Figures 12(a), (b), (c) & (d). The return losses of the array are, for the most part, better than 10 dB over a 2 GHz bandwidth, which is acceptable. A gain of 12 dB is sustained over the 2 GHz bandwidth for the eight-element array. The efficiency of the Vivaldi array has exceeded 75% and only utilizes a $7 \times 7 \text{ in}^2$ real-estate area, as compared to [13] with a $12 \times 18 \text{ in}^2$ area for a similar gain at its center frequency (10 GHz). Note that the conductor loss has been significantly reduced in this case. The reduction in the radiation efficiency is actually due to reflection loss rather than conductor loss. Thus, the array G/T ratio has demonstrated significantly improved values when compared to the one previously developed using Wilkinson power dividers [13]. The G/T value is extremely significant in most UWB applications, where the signal level is generally low, and the noise levels are high due to the associated wide bandwidth.
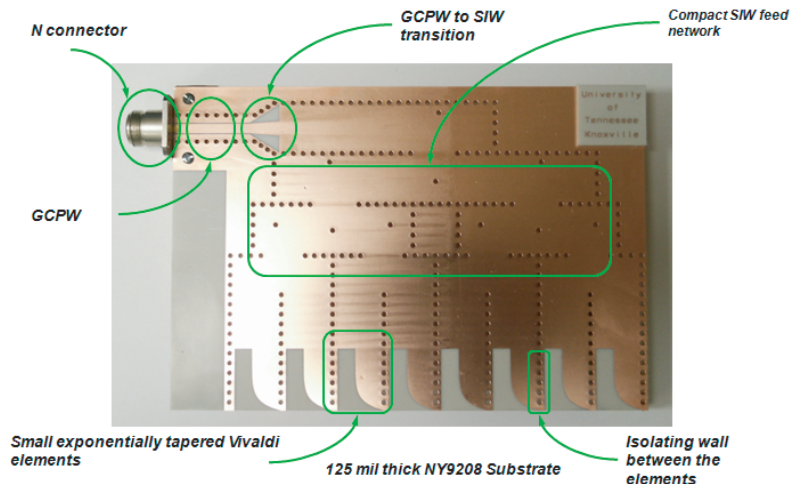

Figure 11. Eight elements Vivaldi array.

E-Plane

7.2 GHz   8 GHz   8.8 GHz

(c)

H-Plane

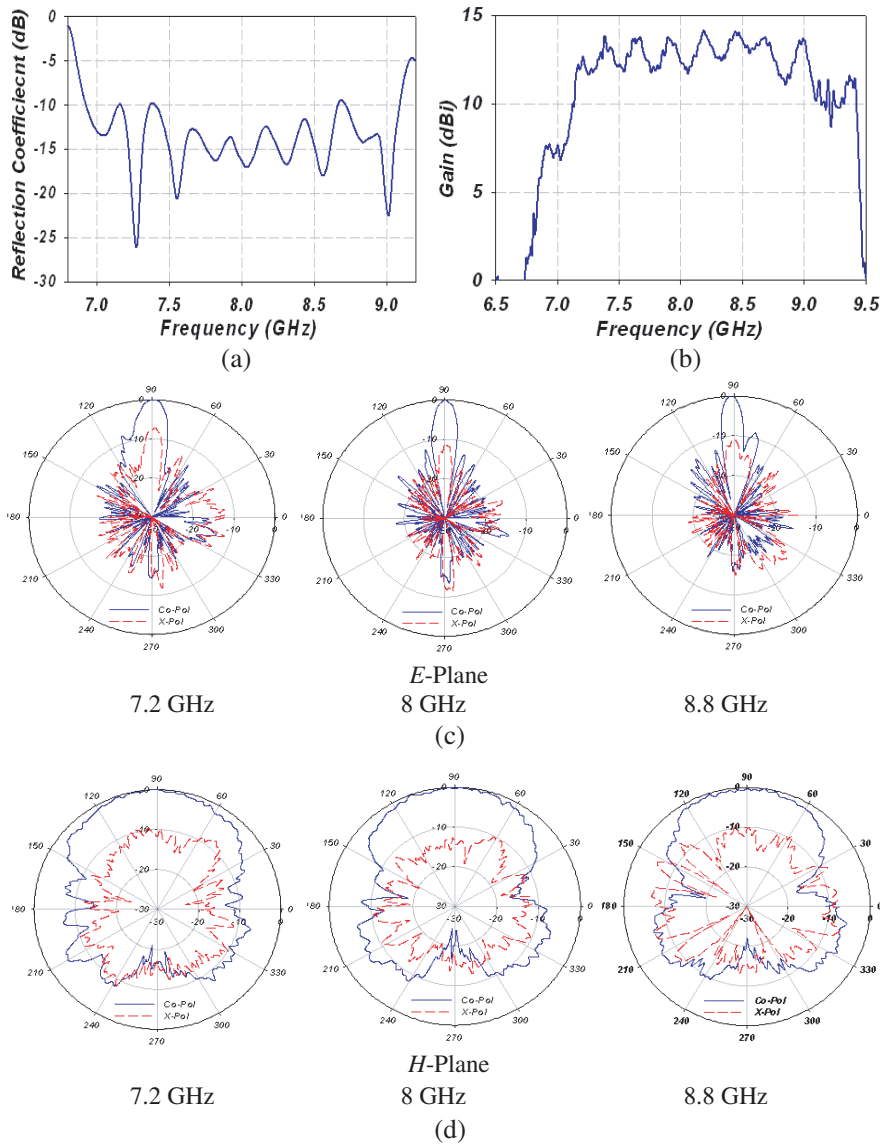7.2 GHz   8 GHz   8.8 GHz

(d)

Figure 12. (a) Reflection coefficient of the array; (b) Gain vs. Frequency; (c) Radiation pattern (*E*-plane) vs. Frequency; (d) Radiation pattern (*H*-plane) vs. Frequency.

7. CONCLUSIONS

Performance of Vivaldi antenna arrays can be enhanced using low-loss feed networks. SIW technology with emulated waveguides can be utilized to minimize such losses, especially when compared to similar structures built using microstrip lines. In our implementation, the SIW structure was optimally designed and fabricated on a thick substrate to minimize the conductor losses, and has led to significant reduction of feed losses. The developed array employs a SIW binary divider to minimize the insertion loss of the feeding network, but it requires the development of a special SIW to GCPW transition to sustain a satisfactory input match while preventing higher order modes excitation over a wide frequency range. Use of optimized T-junctions and the integration of a wideband GCPW feed have led to an even more improved performance with a significant loss reduction.

The developed Vivaldi antenna array has high gain, narrow beam width in the E-plane & H-plane, and a relatively wide bandwidth. The technology is extremely useful for wideband antenna applications such as See-Through-Wall Imaging, Indoor Localization Systems, and Breast Tumor Detection due to its low insertion loss. This technology too can be easily scaled to higher frequencies, even though it will be challenging to add many vias in such close proximity. However, the utilized substrates are much thinner at higher frequencies.

REFERENCES

1. Furuyama, H., Japanese Patent (H4-220881), Jul. 1992.
2. Han, S., X.-L. Wang, Y. Fan, Z. Yang, and Z. He, "The generalized chebyshev substrate integrated waveguide diplexer," *Progress In Electromagnetics Research*, PIER 73, 29–38, 2007.
3. Ismail, A., M. S. Razalli, M. A. Mahdi, R. S. A. Raja Abdullah, N. K. Noordin, and M. F. A. Rasid, "X-band trisection substrate-integrated waveguide quasi-elliptic filter," *Progress In Electromagnetics Research*, PIER 85, 133–145, 2008.
4. Wu, L.-S., R. Wang, and X.-L. Zhou, "Compact folded substrate integrated waveguide cavities and bandpass filter," *Progress In Electromagnetics Research*, PIER 84, 135–147, 2008.
5. Zhang, X.-C., Z.-Y. Yu, and J. Xu, "Novel band-pass substrate integrated waveguide (SIW) filter based on complementary split ring resonators (CSRRS)," *Progress In Electromagnetics Research*, PIER 72, 39–46, 2007.
6. Che, W., E. K.-N. Yung, K. Wu, and X. Nie, "Design investigation

on millimeter-wave ferrite phase shifter in substrate integrated waveguide," *Progress In Electromagnetics Research*, PIER 45, 263–275, 2004.

7. Yang, S. and A. E. Fathy, "Development of a slotted substrate integrated waveguide (SIW) array antennas for mobile DBS application," *Antenna Applications Symposium*, 101–131, IL, 2006.

8. Ansoft HFSS, version 10, ANSYS, Inc..

9. Sang-Gyu, K. and C. Kai, "A low cross-polarized antipodal Vivaldi antenna array for wideband operation," *2004 IEEE Antennas and Propagation Society International Symposium*, Vol. 3, 2269–2272, 2004.

10. Yang, Y. and A. Fathy, "Design and implementation of a low-cost real-time ultra-wide band see-through-wall imaging radar system," *2007 IEEE/MTT-S International Microwave Symposium*, 1467–1470, 2007.

11. Mahfouz, M. R., Z. Cemin, B. C. Merkl, M. J. Kuhn, and A. E. Fathy, "Investigation of high-accuracy indoor 3-D positioning using UWB technology," *IEEE Transactions on Microwave Theory and Techniques*, Vol. 56, 1316–1330, 2008.

12. Salvador, S. and G. Vecchi, "On some experiments with UWB microwave imaging for breast cancer detection," *2007 IEEE Antennas and Propagation Society International Symposium*, 253–256, 2007.

13. Yang, Y., C. Zhang, S. Lin, and A. E. Fathy, "Development of an ultra wideband Vivaldi antenna array," *2005 IEEE Antennas and Propagation Society International Symposium*, Vol. 1A, 606–609, 2005.

14. Cheng, H. Z., H. Wei, L. Hao, Z. Hua, and W. Ke, "Multiway broadband substrate integrated waveguide (SIW) power divider," *2005 IEEE Antennas and Propagation Society International Symposium*, Vol. 1A, 639–642, 2005.

15. Cheng, H. Z., H. Wei, C. J. Xin, C. X. Ping, and W. Ke, "A novel feeding technique for antipodal linearly tapered slot antenna array," *2005 IEEE MTT-S International Microwave Symposium Digest*, 3, 2005.

16. Yang, S. and A. E. Fathy, "Synthesis of an arbitrary power split ratio divider using substrate integrated waveguides," *2007 IEEE/MTT-S International Microwave Symposium*, 427–430, 2007.

17. Deslandes, D. and K. Wu, "Analysis and design of current

probe transition from grounded coplanar to substrate integrated rectangular waveguides," *IEEE Transactions on Microwave Theory and Techniques*, Vol. 53, 2487–2494, 2005.

18. Patrovsky, A., M. Daigle, and K. Wu, "Millimeter-wave wideband transition from CPW to substrate integrated waveguide on electrically thick high-permittivity substrates," *IEEE Microw. Conf.*, 138–141, Oct. 2007.

19. Yang, S., E. Adel, S. Lin, A. E. Fathy, A. Kamel, and H. Elhennawy, "A highly efficient Vivaldi antenna array design on thick substrate and fed by SIW structure with integrated GCPW feed," *2007 IEEE Antennas and Propagation Society International Symposium*, 1985–1988, 2007.

20. Lin, S., S. Yang, and A. E. Fathy, "UWB tapered slot antenna array using siw technology," *Antenna Applications Symposium*, IL, Sep. 2007.

21. Yang, S., S. H. Suleiman, and A. E. Fathy, "Development of a slotted substrate integrated waveguide (SIW) array antennas for mobile DBS," *Proc. Antennas Applications. Symp.*, Montecello, IL, Sep. 2006.

22. Takahashi, T., J. Hirokawa, M. Ando, and N. Goto, "A single-layer power divider for a slotted waveguide array using π-junction with an inductive wall," *IEICE Trans. Commun.*, Vol. E79-B, No. 1, 57–62, Jan. 1996.

23. Fukazawa, K., J. Hirokawa, M. Ando, and N. Goto, "Two-way power divider for partially parallel feed in single layer slotted waveguide arrays," *IEICE Trans. Commun.*, Vol. E81-B, No. 6, 1248–1253, Jun. 1998.

24. Schaubert, D., E. Kollberg, T. Korzeniowski, T. Thungren, J. Johansson, and K. Yngvesson, "Endfire tapered slot antennas on dielectric substrates," *IEEE Transactions on Antennas and Propagation*, Vol. 33, 1392–1400, 1985.